Urban Forestry & Urban Greening 107 (2025) 128776

Contents lists available at ScienceDirect

Urban Forestry & Urban Greening

journal homepage: www.elsevier.com/locate/ufug

Original article

# Adaptive ranking of specific tree species for targeted green infrastructure intervention in response to urban hazards

Xinyu Dong [a,b,c,*], Yanmei Ye [c,**], Dan Su [c], Shengao Yi [d], Runjia Yang [c], Dagmar Haase [a,b], Angela Lausch [a,b,e,f]

[a] Department of Computational Landscape Ecology, Helmholtz Centre for Environmental Research–UFZ, Leipzig 04318, Germany
[b] Landscape Ecology Lab, Geography Department, Humboldt-Universität zu Berlin, Berlin 10099, Germany
[c] Department of Land Management, Zhejiang University, Hangzhou 310058, China
[d] Department of City and Regional Planning, University of Pennsylvania, Philadelphia, PA 19104, USA
[e] Department of Physical Geography and Geoecology, Martin Luther University Halle-Wittenberg, Halle 06120, Germany
[f] Department of Architecture, Facility Management and Geoinformation, Anhalt University of Applied Sciences, Dessau 06846, Germany

ARTICLE INFO

*Keywords:*
Green infrastructure planning
Nature-based solutions
Decision-making
i-Tree Eco model
Urban hazards
Multifunctionality

ABSTRACT

Green infrastructure (GI), with its multifarious benefits, can effectively address urban hazards and enhance urban resilience and sustainability. While traditional GI planning studies incorporate its multifunctionality, they are often limited to identifying prioritized locations for GI intervention without exploring how to respond to the local specific demands. In this study, using a highly urbanized city, Zhengzhou as a case, we first spatially identified urban hazards in three aspects, including urban flood susceptibility, urban heat environment, and air pollution, utilizing machine learning, remote sensing retrieval. Subsequently, we employed the i-Tree Eco model to quantify the effectiveness of potential tree species in unitary functional units in addressing these urban hazards. An adaptive ranking approach was then proposed to match the effectiveness of tree species with local demands for addressing urban hazards. Our results indicate that the inner city area, as well as the northwest should be prioritized for GI interventions. Urban hazards exhibit significant spatial heterogeneity and different tree species also have specific advantages, highlighting the importance of adaptive decision-making. The study area is divided into three zones, and we suggest targeting urban hazards with the most effective GI intervention and maximizing carbon sequestration potential in areas without pronounced urban hazards. The developed framework can serve as guidance for scientific decision-making in urban greening projects.

## 1. Introduction

There is a global trend of consistent urban population growth. As of 2018, approximately 55 % of the population resided in urban areas, and this proportion is expected to rise to 68 % by 2050. This phenomenon is more widespread in China along with the economic boom over the past decades. Chinese cities have expanded drastically (Liu et al., 2016), and it is reported that 17 Chinese agglomerations have experienced an average triple increase in urban size during 1978–2010 (Schneider and Mertes, 2014). Expanding urban boundary inevitably have encroached on other vegetation covers, leading to a series of urban ecological problems, including urban heat island, haze and flooding risk, etc. (Yang et al., 2019). Green infrastructure (GI) has been widely recognized as an efficient solution for addressing urban hazards and improving urban resilience (Korkou et al., 2023). GI purveys multifarious benefits also called multifunctionality, including but not limited to microclimate regulation, stormwater management and air quality improvement (Cook et al., 2024). In this context, scholars have consistently promoted GI as a means to achieve the United Nations Sustainable Development Goals amid growing urbanization and climate change (Lombardía and Gómez-Villarino, 2023; Lu et al., 2024).

This initiative has been substantially endorsed in China, where the development model has shifted to ecological civilization that advocates harmony between humans and nature (Dong et al., 2023a; Zhao et al., 2023b; Zhou et al., 2021). As a result, local governments in most Chinese cities have proposed and implemented numerous greening projects, such

* Corresponding author at: Department of Computational Landscape Ecology, Helmholtz Centre for Environmental Research–UFZ, Leipzig 04318, Germany.
** Corresponding author.
*E-mail addresses:* xinyu.dong@ufz.de (X. Dong), yeyanmei@zju.edu.cn (Y. Ye).

https://doi.org/10.1016/j.ufug.2025.128776
Received 3 November 2024; Received in revised form 11 March 2025; Accepted 11 March 2025
Available online 15 March 2025

as forest cities, garden cities, and sponge cities (Liao et al., 2021; Yin et al., 2021). Li et al. (2021) studied 107 Chinese cities and found that 65 % of long-term built-up areas showed a greener trend from 2010 to 2019. A similar pattern was confirmed by Zhang et al. (2023) who identified that the central areas of most Chinese cities have tended to become greener due to investments in GI. It is evident that these GI developments have achieved some success, making cities greener and mitigating urban problems such as the urban heat island and air pollution.

Given the crucial role of GI, the question of how it should be planned to maximize its multifarious benefits has garnered significant attention from scholars, urban planners, and policymakers (Dong et al., 2023b; Korkou et al., 2023). Although its multifunctionality has been widely recognized, many existing GI planning studies still seem not to fully embrace this feature. For example, multi-objective optimization coupling hydrological models is most frequently applied to optimize its stormwater management performance, and this approach is primarily limited to the community scale rather than the city scale (Leng et al., 2024). Given these shortcomings, Meerow and Newell (2017) first developed a GIS-based green infrastructure spatial planning model, namely GISP in order to capture the multifunctionality. This model becomes a paradigm for subsequent GI planning studies involving multi-benefits analysis (Chang et al., 2021; Rainey et al., 2022). These GIS-based approaches identify the prioritized locations for GI intervention by the spatial differences of regional ecological conditions: the principle of spatial equity. Specifically, since GI can regulate the surrounding microclimate, if a certain area is suffering from a more severe urban heat, the area should be prioritized for GI intervention over other locations without urban heat issues. The overall priority can be obtained by integrating multiple single GI priority layers (Dong et al., 2023b). However, despite being scalable to the city scale, such frameworks resemble land suitability assessments more than integrative GI planning, as they do not directly relate to GI elements. Additionally, these studies are generally limited to priority identification and do not explore further actions for addressing urban hazards (Chen et al., 2022; Goodspeed et al., 2021).

Trees are essential providers of ecosystem services within GI, and different species-specific trees may have various effectiveness in improving surrounding ecological conditions (Ristorini et al., 2023). For example, Manzini et al. (2023) evaluated the performance of 211 trees, and suggested that *Pseudotsuga menziesii* is the best for purifying air quality but is not effective in carbon sequestration, while *Eucalyptus viminalis* demonstrates the opposite effectiveness. Oshio et al. (2021) demonstrated that the quantity of leaves is the predominant factor impacting microclimate regulation capacity of trees, and *Zelkova serrata* can provide more cooling services than *Cinnamomum camphora*.

In practice, the Chinese government launched a notice on scientific GI planning in 2021, which particularly highlights the scientific selection of tree species to accommodate regional conditions so as to maximize the benefits of GI. However, methods for the scientific GI planning, especially linking the effectiveness of tree species with the locally specific demands, are still insufficient. As mentioned above, the performance of stormwater management is given disproportionate attention; although a few studies involve the multi-benefits, they are only limited to identifying the prioritized locations (Chen et al., 2022; Meerow, 2020). Considering the different effectiveness of tree species and various priority for GI intervention, the scientific GI planning should consider the adaptability between the two in order to ensure that the right GI can be targeted in the right places.

Consequently, based on these research gaps, this study aims to propose a novel framework for GI planning, which links the effectiveness of species-specific trees with the local demands by adaptive ranking approach. This study has three advantages over traditional GI planning: (1) conducted on a large scale, covering the whole urbanized area of a city; (2) integrating multi-urban hazards and corresponding benefits of GI (3) not limited to priority identification, further recommending the most matching tree species for each location.

To achieve the above goals, we first quantified the urban hazards, including flood susceptibility, urban heat environment and air pollution utilizing machine learning and remote sensing retrieval. Then, the corresponding effectiveness of species-specific trees was simulated using the i-Tree Eco model. We developed a novel adaptive ranking approach to match the effectiveness of tree species with the locally specific demands for targeted GI intervention. A case study was designed in a populous Chinese city, Zhengzhou, to demonstrate how the adaptive ranking approach recommends the tree species for each location.

## 2. Materials and methods

### 2.1. Study area

Zhengzhou is a megacity located in central China (Fig. 1), as well as the demarcation point between the middle and lower reaches of the Yellow River basin. The city experiences a warm temperate continental monsoon climate, with an average annual precipitation of 632.8 mm. Zhengzhou has four distinct seasons; in summer, the highest air temperature can exceed 40°C, while in winter, the lowest air temperature typically falls below 0°C. As one of the nine national central cities, Zhengzhou experienced a drastic expansion, and the trend is continuing. Official statistics indicate that the urbanized area in the main city surged from 133.2 $km^2$ to 709.69 $km^2$ over the past two decades (2000–2020); the population also spiraled from 6.6 million to 12.6 million. Nevertheless, rapid development and urban sprawl arise a range of urban problems, such as haze, urban heat island and urban flooding (Wang et al., 2019; Yang et al., 2024). Especially in the context of climate change, Zhengzhou has also experienced extreme weather in recent years, including extreme rainfall and extreme heat waves (Guo et al., 2023; Li et al., 2022). These combined issues pose significant challenges to the city's resilience and sustainability.

The locations and boundary of the study area are shown in Fig. 1. The basic assessment unit is 0.25 $km^2$ grids. This study mainly focuses on the continuous urbanized areas of the main city and its immediate surrounding, totally covering 1719 $km^2$, comprising 6876 grids. In Chinese cities, the ring roads often correlate with urbanization intensity. Moving from the inner ring road outward, the intensity generally decreases. The area within or immediately surrounding the inner ring road is typically considered the inner city, while the other parts beyond that are regarded as the outskirts.

### 2.2. Methodology

Traditional GI planning studies usually identify the priority locations for GI intervention based on the spatial differences of urban hazards, namely spatial equity. For example, since GI can regulate air quality and microclimate, areas that suffer from worse air quality and urban heat should be prioritized for GI. To reflect the multifunctionality of GI, the overall priority score is typically obtained by overlaying multiple single-priority maps. These traditional GI planning studies are more akin to land suitability assessments as they indirectly infer GI planning locations rather than directly relate to GI elements. This study further quantifies the effectiveness of species-specific trees using the i-Tree Eco model and ranks the adaptability of tree species for each specific location. Based on this step, we can further determine which tree species is the most recommended for GI intervention to match the local specific demands.

The methodological framework of this study is shown in Fig. 2, which comprises four components. In the first step, we quantified flood susceptibility, urban heat environment and air pollution using machine learning and remote sensing retrieval on 0.25 $km^2$ grids. These urban hazards were converted to corresponding GI demands in terms of spatial equity. Then, the overall priority map was determined by overlaying each single demand map. Traditional GI planning studies usually stop at this point.

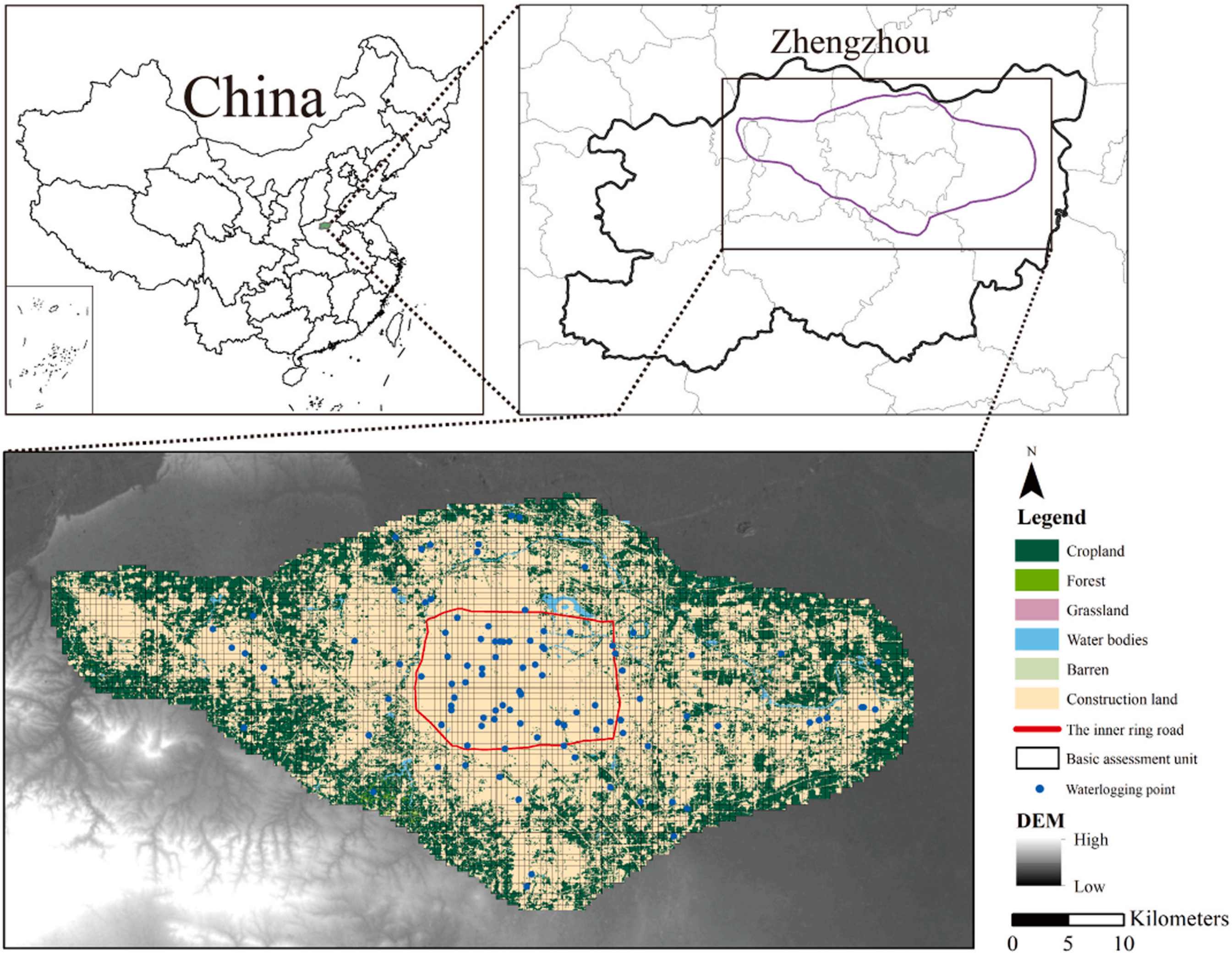


**Fig. 1.** Location and boundary of the study area.

The second component involves quantifying the effectiveness of species-specific trees by the i-Tree Eco model. The effectiveness of tree species was then converted to unitary functional units for a uniform comparison. In the final step, we used an adaptive ranking approach to match the effectiveness of tree species with the local specific demands, ensuring that the right urban trees can be targeted in the right places to effectively address urban hazards. Each component described in Fig. 2 will be expounded in the following sections. All applied data and their sources can be found in Appendix. S1.

### 2.3. Quantification of urban hazards

#### 2.3.1. Urban flood susceptibility

Stormwater management is one of the most emphasized benefits of GI. Traditional GI planning studies usually utilize runoff or impervious ratio to locate prioritized areas (Tran et al., 2020). However, urban areas with more runoff may not necessarily experience waterlogging due to the presence of drainage systems and topographical factors (Cook and Merwade, 2009; Getirana et al., 2023). In practice, runoff-related indicators differ from land surface temperature (LST) or air pollutant concentration, which directly indicate the need for urban heat mitigation and air quality improvement; the latter two represent actual urban hazards, whereas runoff is only an intermediate variable or contributing factor to urban waterlogging (Pugliese Viloria et al., 2024). Therefore, this study uses flood susceptibility to assess the need for stormwater management.

Machine learning has been applied to evaluate urban flooding problems, offering powerful tools to analyze flood susceptibility in complex urban environments. Among these models, support vector machine (SVM) was applied given its strong classification ability, robustness against noise and nonlinear modeling capability (Asaly et al., 2023).

During heavy rainfall, the local transportation department notifies residents of urban waterlogging locations, advising them to avoid these areas if possible. We crawled the website to collect the official announcement regarding locations of all hazardous areas—totally 124—in July 2024 that is the rainy season in Zhengzhou. The locations were given as simply text descriptions in Chinese without coordinates, so we used Python to connect to the Amap API to convert the descriptions into precise latitude and longitude coordinates. These waterlogging areas are shown in Fig. 1.

To improve the performance of SVM, a balanced dataset was applied. We used Python's random sample function to randomly select 124 unique un-flooded samples, and then assigned the waterlogging areas as positive classification (value 1) and the un-flooded areas as negative classification (value 0). We selected seven features, including TWI (topographic wetness index), DEM, slope, aspect, land use, road density and NDVI to train the model as Eq. (1). Before model fitting, the variance inflation factors (VIFs) of the seven features were calculated using Statsmodels to check for multicollinearity. The result indicated that all

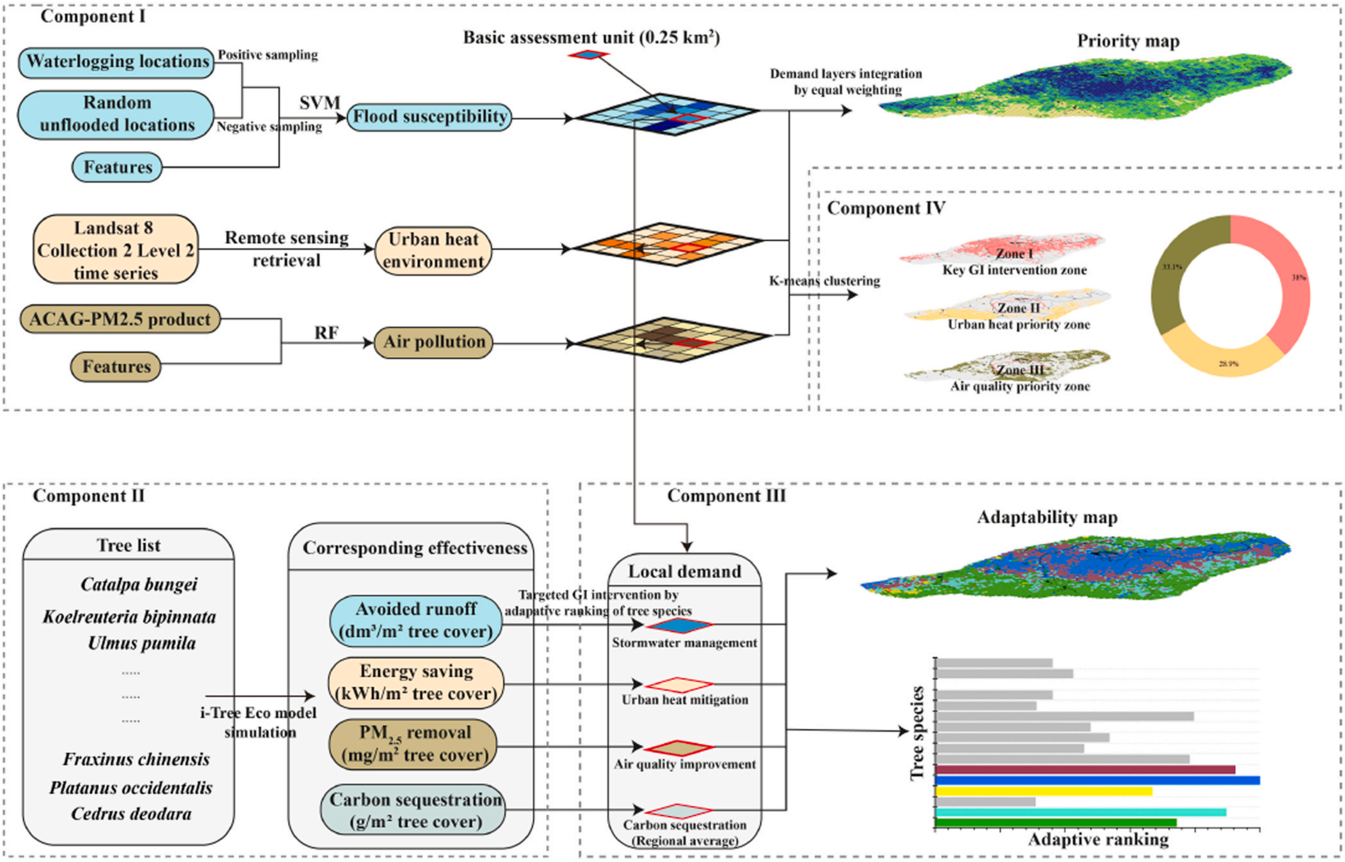


**Fig. 2.** Methodological framework.

seven variables can be retained (VIF<10).

$$Y = SVM(TWI, DEM, slope, aspect, landuse, roaddensity, NDVI) \quad (1)$$

where $Y$ is the classification result, which is a binary value (1 for waterlogging, 0 for non-flooded).

Hyperparameter tuning and 5-fold cross-validation were used to optimize model performance. We set up a hyperparameter grid, with four potential values for C, six potential values for gamma, and three kernel types. Using GridSearchCV, we explored various parameter combinations and performed 360 fittings. It was finally determined that with C= 1, gamma= 0.01 and kernel= RBF, the area under the receiver operating characteristic curve of the model's training set and validation set were 0.93 and 0.89, respectively, which demonstrated acceptable classification accuracy.

GI provides local regulating service for stormwater management, and according to the spatial equity, the higher the flood susceptibility in a specific location, the greater the demand for GI intervention. The value was positively normalized to the 0–1 scale for uniform comparison. The data source applied for quantifying urban flood susceptibility can be found in Appendix. S1.

### *2.3.2. Uban heat environment*

Since GI can effectively regulate the surrounding microclimate and address urban heat hazards, previous GI planning studies often used LST to determine the priority location for urban heat mitigation (Korkou et al., 2023; Wang et al., 2021). Martilli et al. (2020) also suggested that using LST in heat mitigation studies, as it is the most direct metric. This study applies LST to represent urban heat environment, and assesses the urgency for GI intervention based on its spatial difference. The United States Geological Survey (USGS) launched the Landsat Collection 2 Level 2 dataset in 2020, which is atmospherically corrected. This product is advantageous in LST retrieval compared to traditional methods, such as the single-channel algorithm and radiative transfer equation, which requires numerous auxiliary atmospheric parameters (Sekertekin and Bonafoni, 2020).

In order to capture the urban heat condition for the whole year, we retrieved all Landsat 8 imageries in 2022 using Google Earth Engine. We only assessed the cloud contamination within the study area in order to retain as many images as possible. A cloud-masking function was defined to identify and mask out high-confidence clouds and cloud shadows using specific bits in the quality-assessment band. We then counted the number of cloud pixels and the total pixels within the study area using the Reduce Region method, and retained images with a ratio of cloud pixels to total pixels below 5 %. Next, the LST was retrieved from each image using a multiplicative scale factor and offset in accordance with USGS guide (USGS, 2024). To reflect the most hazardous urban heat for the entire year, we composited the maximum value of the LST time series. The higher the LST in a specific location, the greater the need for GI to regulate the microclimate. The LST value also was normalized to allow uniform comparison with other demand layers.

### *2.3.3. Air pollution*

The capacity of GI to absorb ambient air pollutants is well-established (Ristorini et al., 2023). Due to the significant health impacts of fine particulate matter ($PM_{2.5}$), it is often prioritized for monitoring and mitigation (Maji et al., 2023). In this study, we used $PM_{2.5}$ concentration as an indicator to assess local demands for air quality improvement, following the approach commonly adopted in previous GI planning studies (Chang et al., 2021; Meerow, 2019).

Due to the sparse distribution of air monitoring stations, it is difficult to map $PM_{2.5}$ concentration using the monitoring data at a fine resolution. The ACAG-$PM_{2.5}$ product is a remote sensing-derived dataset released by Shen et al. (2024). It estimates $PM_{2.5}$ by combining satellite-based aerosol optical depth (AOD) with the GEOS-Chem chemical transport model, then adjusts the results with ground-based measurements. This product was utilized in our study as it offers a detailed spatial distribution of $PM_{2.5}$ concentrations, enabling the identification of areas suffering from worse air quality. The resolution of the dataset, however, is 0.01°, which does not match with the basic assessment unit. We further downscaled it using random forest regression, following Yang et al. (2020).

We used five features, including DEM, land use, MODIS-AOD MCD19A2 550 nm and coordinates ($x$ and $y$) to fit the non-linear model. All features were first resampled to the resolution of 0.01° to match the simulated $PM_{2.5}$ dataset. Before fitting the model, VIFs for the five input variables were calculated with Statsmodels to assess multicollinearity. Results showed that all five variables could be retained, as each had a VIF below 10. Then, a complex non-linear regression model with the five features and the ACAG-$PM_{2.5}$ concentration as the response variable was established as described in Eq. (2)

$$PM_{2.5} = RF(DEM, AOD, landuse, lat, lon) \tag{2}$$

where $PM_{2.5}$ is the ACAG-$PM_{2.5}$ concentration; $lat$ and $lon$ are the coordinate of each grid.

Hyperparameter tuning and 5-fold cross-validation were also applied to improve the model accuracy. We set up a hyperparameter grid using GridSearchCV, with five potential values for the number of trees, six potential values for the maximum depth of each tree, eight potential values for the minimum number of samples required to split and to be at a leaf node, and two options for bootstrap. A total of 4800 fittings were performed, and the coefficient of determination ($R^2$) of the model's training set and validation set were 0.88 and 0.86 under optimal parameters of 200, 20, 2, 1, and True, which demonstrated desirable predicative accuracy.

After the nonlinear model fitting, we then resampled these features to a resolution of 500 m to match the basic assessment unit. The resampled features were then input into the model to downscale $PM_{2.5}$ concentrations to a finer resolution. Areas with higher $PM_{2.5}$ concentrations were assigned greater priority for air quality improvement. The $PM_{2.5}$ values were also normalized for consistent comparison with other demand layers.

#### 2.3.4. Priority ranking

Existing GI planning studies typically determine the overall priority for GI intervention by combining each demand layer using different weighting methods, such as equal weighting, dynamic weighting, and stakeholder preference weighting (Chen et al., 2022; Tran et al., 2020). These weighting methods have been thoroughly studied and each offers distinct advantages. Since this study introduces an adaptive ranking approach for targeted GI intervention, we focus on the degree of matching between the effectiveness of tree species and the local demands. Therefore, we integrated each demand layer using the commonly applied equal weighting method. The overall priority for GI intervention is then determined by Eq. (3).

$$P_i = \sum_{j=1}^{3} w_{ij} \tag{3}$$

where $P_i$ is the overall priority for GI intervention on the $i$th location; $w_{ij}$ is the $j$th demand on the $i$th location.

### 2.4. Quantification of benefits of GI

#### 2.4.1. Tree list for GI intervention

The local government formulated the Forest Zhengzhou Ecological Development Plan (2020–2035) and issued a recommendation for plant species, which limits the range of species for subsequent greening projects. This recommendation list includes thirty different species, but almost a half are flowers and shrubs such as *Prunus triloba*, *Rosa chinensis*, and *Buxus megistophylla*. However, owing to structural attributes, such as large crowns and extensive root systems, and biological traits like long life cycles and substantial biomass, trees are generally more effective than smaller vegetation at capturing air pollutants, regulating microclimates, and storing carbon (Zhao et al., 2023a). Therefore, this study mainly focuses on these tree species from the list as the potential GI intervention measure to respond to the local demands.

#### 2.4.2. i-tree ECO model simulation

The latest version (6) of the i-Tree Eco model can assess and differentiate the environmental benefits of different species of trees and shrubs. Since the first release of the i-Tree Tools in 2006 (i-Tree, 2024), the model has been extensively used in studies evaluating the effectiveness of species-specific GI (Yao et al., 2022). Its accuracy and reliability have been demonstrated. Using local meteorological and pollution data, we applied this model to simulate the effectiveness of specific tree species in avoiding runoff, saving building energy, removing air pollution, and sequestering carbon. Notably, since the benefits of GI in regulating the microclimate are less easily quantifiable compared to runoff control and air purification, building energy savings could be a proxy to indicate the effectiveness of GI in mitigating the urban heat island effect (Morakinyo et al., 2018). Therefore, the first three benefits could address the local issues, which corresponds to the urban hazards quantified in the previous section, while carbon sequestration provides a significant global benefit in mitigating climate change. Nevertheless, trees may provide more ecological benefits due to a larger footprint rather than just their specific properties (Salmond et al., 2016). In highly urbanized areas, the space for greening projects is usually limited. To accommodate this actual planning situation, we utilized an equal-area-based functional unit (as shown in Table 1) to distinguish the effectiveness of tree species (Nyelele et al., 2022). The higher the functional unit effectiveness of a tree, the greater the ecological improvement that can be achieved for the same amount of green coverage.

#### 2.4.3. Parameters setting

The model requires various tree properties, including tree species, height, diameter at breast height (DBH), canopy width, and cover (Riondato et al., 2020). Of these, tree species and DBH are mandatory because these two parameters directly influence the ecological and growth characteristics. Other trait parameters can be estimated by the model using allometric equations or empirical formulas within the i-Tree database. This is a planning-oriented study, with the primary objective of differentiating the effectiveness of species-specific trees under standardized conditions, rather than evaluating specific existing trees. As such, we only input the DBH and species, and other parameters were estimated by the database to assume standard morphological characteristics and consistent health condition. Except for flowers and shrubs, there are sixteen tree species on the list, which were directly input into the model. According to the Urban Greening Standards released by the government (MOHURD, 2023), the DBH of newly-planted tree should be lower than 15 cm. In accordance with this mandatory requirement for greening projects in Chinese cities, we set the DBH of the sixteen tree species at 15 cm. We then simulated the effectiveness of species-specific trees. The effectiveness was converted the value to the functional and normalized with respect to the maximum

**Table 1**
Functional unit of benefits.

| | Benefits of green infrastructure | | | |
|---|---|---|---|---|
| | Avoided runoff | Building energy saving | Air pollution removal | Carbon sequestration |
| Functional unit | $dm^3/m^2$ tree cover | $kWh/m^2$ tree cover | $mg/m^2$ tree cover | $g/m^2$ tree cover |

value to a 0–1 interval for uniform comparison and integration across different effectiveness categories.

### 2.5. Targeted GI intervention with adaptive weighting

We developed an adaptive ranking approach to align the effectiveness of species-specific trees with local demands throughout the study area. At each location, the weight assigned to a specific effectiveness of trees corresponds to the local demand for GI intervention at that site. In addition to benefits that respond to local demands, we also consider the carbon sequestration. However, this large-scale effect primarily contributes to climate change mitigation; it may not vary significantly within a city, and usually cannot be detected by residents (Tran et al., 2020). This suggests that targeted GI intervention for carbon sequestration may not be necessary at a fine resolution. Therefore, its weight was set as the average of the weights assigned to three locally derived benefits to ensure equal consideration. The targeted GI intervention using adaptive ranking of tree species is presented in Eq. (4).

$$S_{ij} = \sum_{n=1}^{l} w_{in} \times b_{jn} + \frac{\sum_{i=1}^{k}\sum_{n=1}^{l} w_{in}}{k \times l} \times c_j \tag{4}$$

where $S_{ij}$ is the adaptability of the $j$th tree species on the $i$th location; $b_{jn}$ is the $n$th effectiveness of the $j$th species-specific tree; $w_{in}$ is the weighting for the $n$th effectiveness of tree species on the $i$th location, which equals to the $n$th demand on the $i$th location; $c_j$ is the carbon sequestration capacity of the $j$th species-specific tree. All values used for the adaptive ranking were normalized to eliminate dimensional differences.

### 2.6. K-means clustering

Determining the cluster patterns of local demands for GI intervention is essential for developing a zone planning strategy, commonly applied in GI studies and projects (Jia et al., 2022). K-means clustering was used for the spatial analysis of these local demands given its advantages of reliable clustering effectiveness and fast convergence speed. There are three elements for the clustering, including demand for stormwater management, urban heat mitigation and air quality improvement. The clustering result can be obtained when the sum of squared distances is minimized, as expressed in Eq. (5):

$$SSD = \sum_{i=1}^{k}\sum_{q_j \in s_i} \left\| q_j - u_i \right\|^2 \tag{5}$$

where $SSD$ is the sum of squared distances; $k$ is the clustering number; $q_j$ is the grid cells that are classified into $i$th clustering; $u_i$ is the center point of $i$th clustering.

## 3. Results

### 3.1. Identification of urban hazards

The urban hazards in the three aspects and the overall priority that overlays each demand layer are illustrated in Fig. 3(a-e). The Jenks natural break point method was employed to classify these maps into five categories considering that this method can maximize differences between groups and minimize within-group variance, thereby enhancing visualization (Cao et al., 2023).

#### 3.1.1. Urban flood susceptibility

In Fig. 3(a), flood susceptibility shows notable spatial heterogeneity across the city. The highest flood susceptibility levels (above 0.72) are predominantly concentrated within the inner ring road, with some high-susceptibility locations extending into the eastern and northwestern areas. Overall, the inner city displays a high susceptibility to urban flooding, with most areas exhibiting susceptibility levels above 0.55, indicating a substantial need for stormwater management measures. In contrast, the western side of the city generally has lower susceptibility levels than the eastern side. While the western sub-center shows higher susceptibility, many areas in the western part of the city exhibit the lowest flood susceptibility level (below 0.22), suggesting a relatively reduced flood risk. This uneven spatial pattern highlights the importance of targeted GI intervention in high susceptibility areas to mitigate flood hazards effectively.

#### 3.1.2. Urban heat environment

The urban heat environment is illustrated in Fig. 3(b), highlighting a

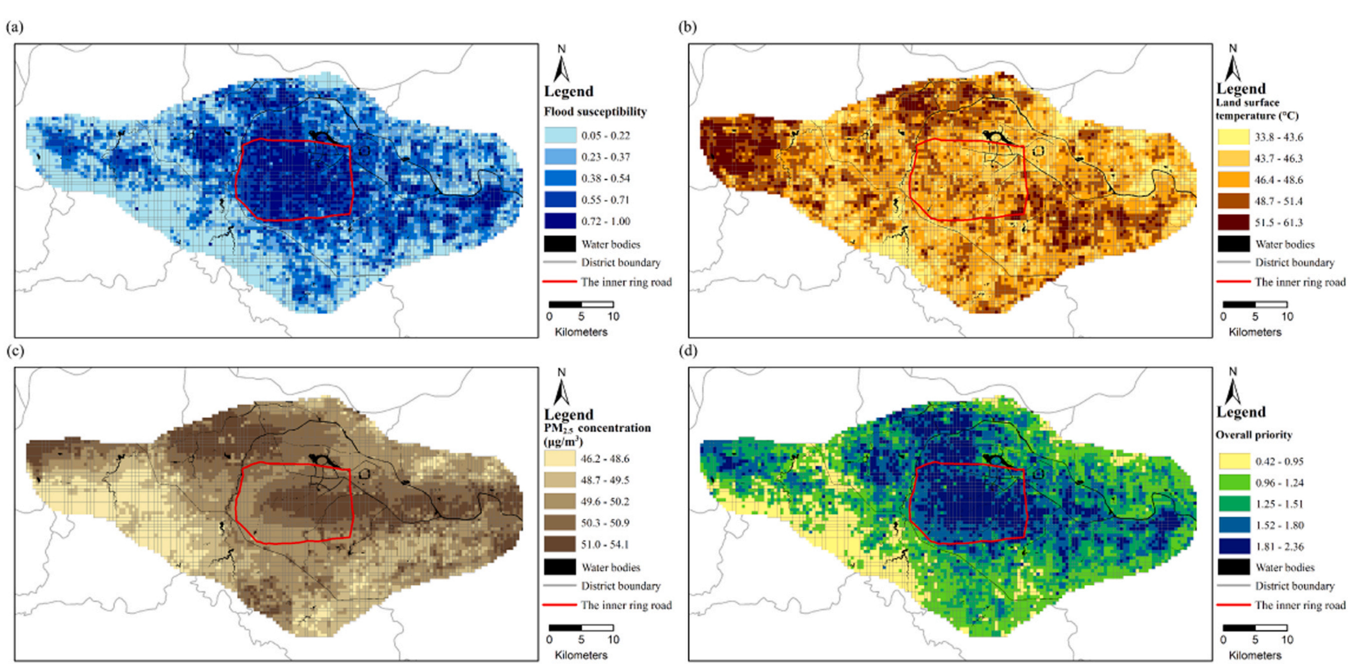


**Fig. 3.** Spatial pattern of urban hazards and overall priority; (a-c) specific urban hazards; (d) overall priority for GI intervention.

notable spatial unevenness. Unlike urban flood susceptibility, the inner city's urban heat environment is more mitigated compared to the periphery. Only a few areas within the inner ring road exhibit the highest urban heat levels. However, the eastern sub-center experiences the most severe urban heat, with many locations in this region showing LST exceeding 51.5°C, suggesting the greater demand for urban heat mitigation. Additionally, certain spots in the northwest and southeast also experience elevated urban heat levels. Overall, three distinct urban heat island clusters are distributed beyond the inner city. The map's black areas represent water bodies, and the LST in these zones is relatively lower, suggesting that blue infrastructure plays a significant role in mitigating urban heat in nearby areas.

#### 3.1.3. Air pollution

Fig. 3(c) reveals the uneven spatial pattern of air pollution. Generally, the air quality within the inner ring road and northwestern end is worse than other regions, and there are most locations with the higher $PM_{2.5}$ concentration of 49.6 μg/m$^3$, indicating the greater demand for air quality improvement. Several areas around the fringe also exhibit severe air pollution, especially in the western and eastern tips. These areas are industrial zones, where a large number of manufacturing enterprises are gathered, potentially contributing to additional air pollution. In comparison, the optimal air quality is observed in the southeast where almost all areas show the lowest $PM_{2.5}$ concentration. Notably, the air pollution in Zhengzhou is very severe, and even in the most favorable area, the $PM_{2.5}$ concentration of 46.2 μg/m$^3$ is higher than the Chinese Standard (below 35 μg/m$^3$), highlighting the urgency to alleviate the urban hazard.

#### 3.1.4. Overall priority for GI intervention

The overall priority for GI intervention that overlays all single demand layers (including demand for stormwater management, urban heat mitigation and air quality improvement) with equal weighting is shown in Fig. 3(d). Overall, locations in the urban core area and northwest should be prioritized for GI intervention where the overall priority level is two or three higher than other areas. A few of the remaining highest priority zones are also scattered across the western and eastern sides. Notably, quarters in the southwest exhibit moderate urban hazards, with almost all areas having the lowest priority for GI intervention. Areas around water bodies and urban parks, such as Longhu Park, are assigned lower priority for GI intervention compared to their surroundings. This underscores the significant role of blue-green infrastructure in improving the ecological conditions of adjacent areas.

### 3.2. Effectiveness of specific tree species

Table 2 shows the tree list and the effectiveness of specific tree species in terms of unitary functional units, under Zhengzhou's meteorological and pollution conditions. *Magnolia grandiflora* is the most efficacious species in $PM_{2.5}$ removal and runoff abatement, capable of purifying 646.7 mg of $PM_{2.5}$ and reducing 12.19 dm$^3$ of runoff per functional unit. *Cedrus deodara* excels in carbon sequestration, storing 1032.8 g of carbon per functional unit. For energy saving, linked to microclimate regulation, *Pinus tabuliformis* is the most advantageous, saving 1186.7 Wh of energy per functional unit. In contrast, *Cornus walteri* is the weakest tree species in three aspects, with 257.2 mg of $PM_{2.5}$ removal, 8.16 dm$^3$ of runoff control, and 415.7 Wh of energy saving per functional unit, respectively. *Ginkgo biloba* is the least effective species in carbon sequestration, capturing only 108.2 g of carbon per functional unit due to its slow growth rate.

Among the sixteen species, some are outperformed by others across multiple benefits. For example, although *Platanus occidentalis* is desirable for stormwater management and microclimate regulation, its effectiveness is dominated by *Fraxinus chinensis* in all four aspects. As a comparatively unfavorable species, *Cornus walteri* is simultaneously dominated by *Cedrus deodara, Fraxinus chinensis*, *Styphnolobium japonicum* and *Ulmus pumila*. This suggests that in locations where space for GI intervention is limited, tree species with lower benefits per functional unit should be avoided when possible. However, aside from these dominated species, others have specific advantages; for instance, while *Cedrus deodara* is superior in carbon sequestration, it is comparatively less effective in stormwater management; *Acer truncatum* is efficient in runoff control and microclimate regulation but incapable in carbon sequestration. In general, *Magnolia grandiflora* offers significant benefits per functional unit, excelling in $PM_{2.5}$ removal and runoff control while also performing well in energy saving.

Overall, the effectiveness of species-specific GI varies widely, underscoring the importance of adaptive decision-making based on locally-specific needs for GI intervention—essentially, planning the right trees in the right places.

### 3.3. Adaptability map

Fig. 4(a) illustrates the most recommended tree species for GI intervention across all assessment units in the area. Fig. 4(b) represents the relative proportion of tree species. Fig. 4(c-e) show cases of adaptive ranking in three different locations with varying demand preferences. It should be noted that the legend applies to all figures, with grey

**Table 2**
Effectiveness of specific tree species.

| | Species | Benefits | | | |
|---|---|---|---|---|---|
| | | $PM_{2.5}$ removal (mg/m$^2$·yr$^{-1}$) | Carbon sequestration (g/m$^2$·yr$^{-1}$) | Avoided runoff (dm$^3$/m$^2$·yr-1) | Energy saving (Wh/m$^2$·yr$^{-1}$) |
| Advantageous species | *Cedrus deodara* | 410.4 | 1032.8 | 9.57 | 712.0 |
| | *Fraxinus chinensis* | 505.1 | 498.6 | 11.41 | 924.1 |
| | *Styphnolobium japonicum* | 301.2 | 556.7 | 8.77 | 796.6 |
| | *Pinus tabuliformis* | 452.2 | 284.0 | 10.13 | 1186.7 |
| | *Magnolia grandiflora* | 646.7 | 378.7 | 12.19 | 777.3 |
| | *Acer truncatum* | 532.9 | 393.0 | 11.74 | 952.1 |
| | *Koelreuteria bipinnata* | 508.8 | 416.3 | 11.42 | 724.8 |
| | *Ulmus pumila* | 407.9 | 526.1 | 10.22 | 423.8 |
| Dominated species | *Platanus occidentalis* | 430.9 | 257.7 | 10.50 | 857.7 |
| | *Pinus bungeana* | 450.5 | 141.2 | 10.09 | 905.6 |
| | *Ligustrum lucidum* | 558.1 | 329.5 | 11.29 | 725.3 |
| | *Eriobotrya japonica* | 360.5 | 587.2 | 9.06 | 444.5 |
| | *Ginkgo biloba* | 391.8 | 108.2 | 9.99 | 902.7 |
| | *Cornus walteri* | 257.2 | 487.1 | 8.16 | 415.7 |
| | *Bischofia polycarpa* | 346.7 | 851.1 | 8.87 | 467.4 |
| | *Catalpa bungei* | 398.5 | 400.8 | 10.09 | 422.5 |

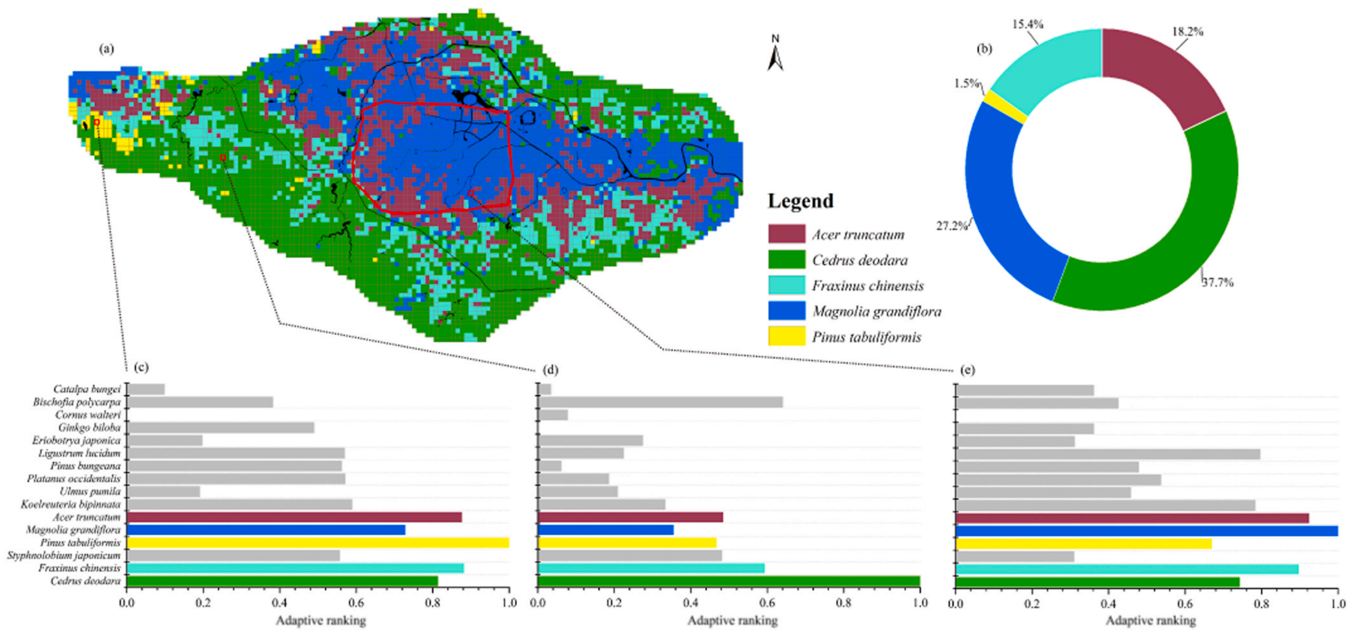


**Fig. 4.** Adaptive ranking map.

representing the dominated tree species in adaptive ranking.

*Cedrus deodara* and *Magnolia grandiflora* are more recommended than other species, matching with 37.7 % and 27.2 % of locations, respectively. These two species form the keystone tree species. The difference is *Magnolia grandiflora* is more adaptive within intra-urban areas while *Cedrus deodara* is more recommended in the periphery. The proportion of *Acer truncatum*, *Fraxinus chinensis*, and *Pinus tabuliformis* accounts for 18.2 %, 15.4 %, and 1.5 %, respectively. These three species are more

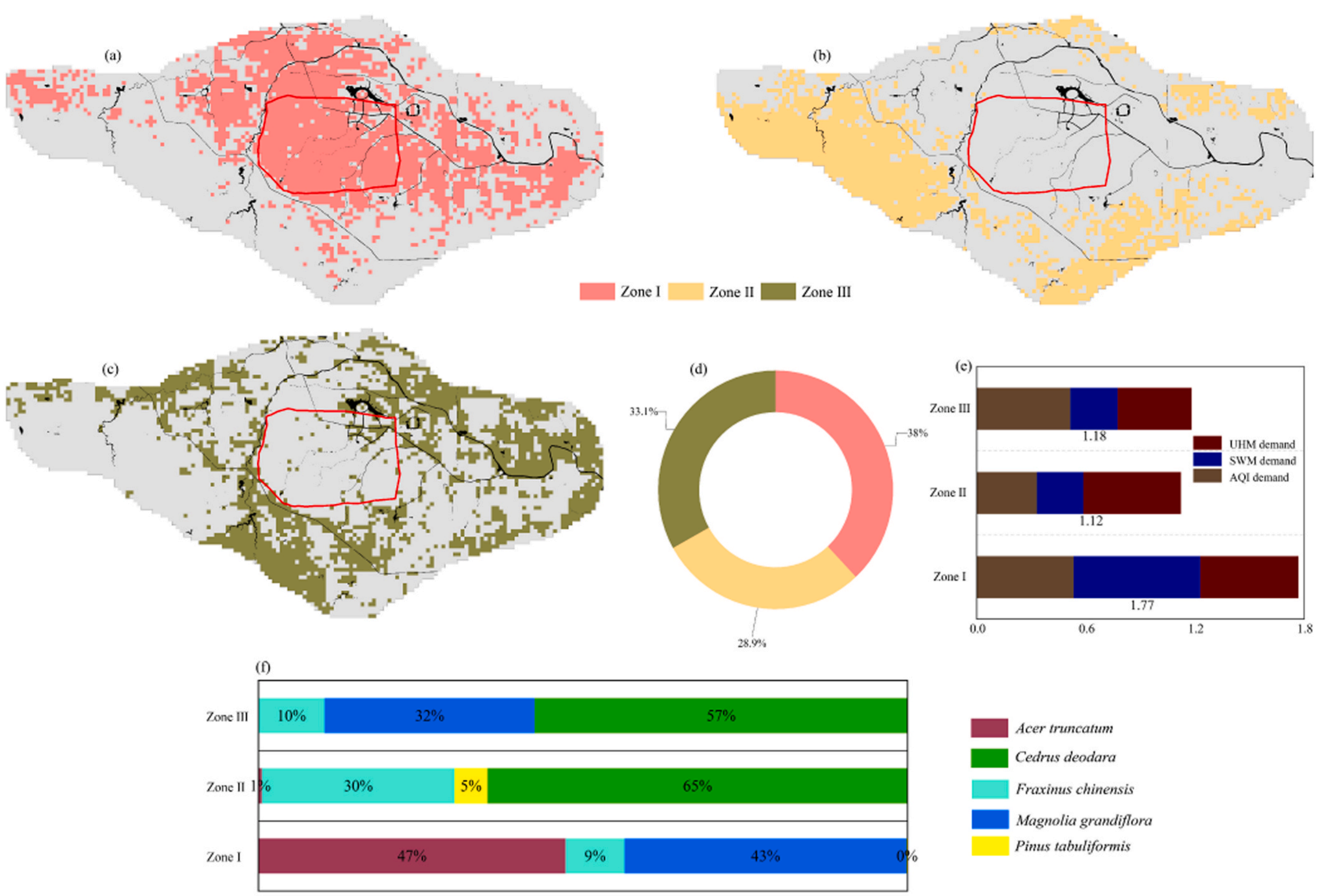


**Fig. 5.** Zoning for GI intervention.

adaptive to different locations. For example, *Acer truncatum* is more recommended in the transitional zone between the inner city and the periphery, while *Fraxinus chinensis* is more suitable for planting immediately surrounding the areas where *Acer truncatum* is recommended. *Pinus tabuliformis,* although the most effective in regulating the microclimate, is the least recommended species, with only 1.5 % of locations experiencing severe urban heat suggested for GI intervention using this species—making its recommendation almost negligible. In addition, although *Ulmus pumila*, *Koelreuteria bipinnata* and *Styphnolobium japonicum* are not dominated by other tree species, no locations are recommended for GI intervention using the three tree species.

Fig. 4(c-e) shows three cases of adaptive ranking to match different local demand preferences. The location in the far west (Fig. 4(c)) faces a higher urban heat hazard, with an urgent need for heat mitigation. In comparison, flood susceptibility and air pollution are less significant in this area, making Pinus tabuliformis the most adaptive tree species for local needs. *Cedrus deodara* ranks highest among the sixteen tree species in the southwest location (Fig. 4(d)), which has favorable conditions across the three urban hazards, resulting in comparatively lower intervention demands. *Cedrus deodara* is therefore optimal, as it provides the most carbon sequestration benefits irrespective of local condition change. The area within the inner ring road (Fig. 4(e)) experiences simultaneous air quality and waterlogging issues, making *Magnolia grandiflora* the most suitable species to respond to the local demand, as it happens to be the most effective in stormwater management and air quality improvement.

### 3.4. Zoning for GI intervention

Fig. 5(a-c) illustrates the spatial patterns of the clustering results obtained through k-means clustering, while Fig. 5(d-f) depicts the proportions of the three intervention zones, their corresponding priorities, and the ratios of the most suitable tree species. Based on the characteristics of the recommended tree species and demand scores, the clustering results were categorized into the key GI intervention zone (zone I), urban heat priority zone (zone II), and air quality priority zone (zone III).

#### 3.4.1. Zone I — key GI Intervention zone

Zone I comprises 38 % of the area, primarily concentrated within the inner city, the north, and the east, with some scattered grids in industrial areas at the western tip. Characterized by high urbanization and poor ecological conditions, this zone faces the most severe urban hazards, including flood susceptibility, urban heat, and air pollution, necessitating effective GI intervention. *Magnolia grandiflora* and *Acer truncatum* perform advantageously in addressing local needs, aligning well with regional conditions. Nearly 91 % of the areas in this zone are recommended for intervention with these two species. Given the highest average priority score of 1.77, this area is identified as the key GI intervention zone, where urban hazards are most severe, and intervention should prioritize local demands.

#### 3.4.2. Zone II — urban heat priority zone

Zone II covers 28.9 % of the total area, mainly aggregated in the west and the southeast. The urban heat environment in this zone is nearly as severe as in the key GI intervention zone, highlighting the urgency for urban heat mitigation. However, the demands for stormwater management and air quality improvement are comparatively moderate. The most suitable species are *Cedrus deodara* and *Fraxinus chinensis*, covering 65 % and 30 % of the zone, respectively. These species are particularly effective in microclimate regulation and carbon sequestration, aligning well with regional needs. With the lowest average overall priority score of 1.12 but a relatively higher demand for urban heat mitigation, this zone is designated as the urban heat priority zone, focusing on improving thermal conditions. However, in areas without prominent urban hazards, it should be considered to maximize urban carbon sequestration capacity.

#### 3.4.3. Zone III — air quality priority zone

Zone III encompasses 33.1 % of the total area, primarily located around the southwest and the northeast, with a few sections inside the inner city. The predominant urban hazard in this zone is air pollution, which is nearly as severe as in the key GI intervention area, while the demands for stormwater management and urban heat mitigation are of lower priority. *Cedrus deodara* and *Magnolia grandiflora* are the most suitable tree species, covering more than 90 % of the zone. The ecological conditions here are relatively favorable, with a lower average priority score of 1.18, positioning it as a suitable space for maximizing carbon sequestration capacity, similar to Zone II. However, specific attention should be given to air pollution control, thus designating this zone as the air quality priority zone.

## 4. Discussion

### 4.1. Comparison with previous studies

Given the significant potential of GI in enhancing urban resilience and sustainability, GI planning research has become a focal point in recent years (Corgo et al., 2024; Van Oijstaeijen et al., 2020). However, traditional studies have notable limitations. Firstly, they are often single-benefit oriented, focusing on a specific aspect such as stormwater management or urban heat island mitigation (Aydin et al., 2024; Camacho-Caballero et al., 2024; Dong et al., 2023c). Since this narrow focus neglects the multifunctionality that is a key characteristic of GI, the final planning implications may hinder the achievement of other benefits (Alves et al., 2024). Additionally, many planning cases are typically conducted at the community level using locally-specific data, making them difficult to replicate in other regions and scale up to the whole-city level.

Meerow and Newell (2017) proposed a GISP model for GI planning, and the multifaced benefits of GI are emphasized. However, these models are limited to the identification of prioritized locations. Specifically, due to the benefit of microclimate regulation, areas with more severe thermal condition are given higher priority for GI intervention (Chen et al., 2022; Dong et al., 2023b). Such studies do not involve GI elements but rather infer the prioritized locations indirectly based on the spatial difference of local conditions corresponding to GI benefits. This underlying logic makes them not a complete GI planning and more akin to land suitability assessments. Although a few studies have attempted to match GI with regional demands, the effectiveness of GI is simply inferred from literature reviews, which amplifies uncertainty (Jia et al., 2022). Furthermore, GI in such studies refers to specific engineering infrastructures, whereas the ecological benefits of GI are actually provided by particular plant within the engineering infrastructures. For instance, a rain garden that is usually considered as GI could have varying ecological performance depending on the plant species it contains (Bruner et al., 2023). Thus, it is misleading to link GI directly to ecological benefits when simply considering it as a specific engineering facility.

In light of previous limitations, this study proposes an adaptive ranking approach linking the effectiveness of tree species to local demands for targeted GI intervention. We first identified the multifaceted demands for GI intervention based on the principle of spatial equity, and then overlaid all demand layers to determine the overall priority. Traditional GI planning studies often stop at this point. Additionally, traditional GI planning studies often use runoff as a criterion for assessing local demand for stormwater management (Meerow and Newell, 2017; Tran et al., 2020). However, due to the influence of urban drainage systems and terrain, runoff is not equivalent to presentation of waterlogging. Comparatively, this study uses flood susceptibility as an alternative to rainfall runoff to better reflect urban hazards.

Based on the identification of local demands, we further used the i-

Tree Eco model to quantify the effectiveness of specific tree species under local meteorological and pollution conditions using unitary functional units, namely per square meter of tree cover. Given that space for GI development in highly urbanized areas is usually limited, introducing this unified functional unit provides a novel solution to accurately capture the real effectiveness of GI within the given green coverage goal (Nyelele et al., 2022). Building on the second component, this study applies the adaptive ranking approach to match the effectiveness of tree species with the local demands in each assessment unit. Through this linkage, this study not only identifies prioritized intervention locations, as seen in traditional GI planning studies, but also determines which tree species should receive preferential treatment in each location to better address local specific urban hazards. Furthermore, we conducted this study in a populous Chinese city, covering more than 1700 $km^2$. Despite the large area, the resolution was refined at 0.25 $km^2$ grids. Thus, this study represents an improvement in both research scale and resolution (Meerow, 2019; Sarabi et al., 2022).

In addition, this study primarily applies open-source data, such as remote sensing data and the $PM_{2.5}$ dataset. The i-Tree ECO model also supports most cities globally, which enhances the replicability. Although the flood points are specifically recorded by the Zhengzhou municipal department, for cities without flood records, remote sensing data, such as polarization data from Sentinel-1 satellite's synthetic aperture radar imagery, can serve as an alternative to extract flood-prone areas (Zhu et al., 2024).

### 4.2. Planning implications

In accordance with the adaptive ranking of tree species in each assessment unit as well as the k-means clustering results, we propose two GI intervention strategies.

#### 4.2.1. Planning strategies I: targeting urban hazards with the most effective GI

In practice, urban greening projects often focus more on increasing green space coverage and less on optimizing other critical elements (Li et al., 2023). However, the effectiveness of different tree species varies greatly. For example, *Magnolia grandiflora* provides more than twice the $PM_{2.5}$ removal capacity compared to *Cornus walteri*, but its microclimate regulation function is less effective than that of *Fraxinus chinensis*. If these differences are disregarded, the actual ecological improvements may vary significantly, even under the same green coverage. We suggest that scientific urban greening projects should not merely pursue an increase in green coverage but rather focus on efficiency. Targeting local specific demands with the most adaptive tree species can simultaneously increase the green coverage, enhance urban ecological conditions and efficiently address the inequitable distribution of urban hazards. Additionally, it is important to optimize other elements such as spatial distribution, landscape patterns during GI intervention to further improve the connectivity and cooling effects (Ortega et al., 2023; Xu et al., 2024). Therefore, we propose the first strategy for GI intervention: targeting urban hazards with the most effective GI. The adaptive ranking of tree species to match locally specific demands provides a practical pathway for this consideration. The spaces for urban greening projects are usually limited, especially within highly urbanized areas. Targeting urban hazards with the most effective GI can enhance urban ecological quality as much as possible within the same green coverage goal.

#### 4.2.2. Planning strategies II: maximizing carbon sequestration potential in areas without pronounced urban hazards

GI removes $CO_2$ from the atmosphere through photosynthesis, storing it in vegetation and soil, which is crucial for climate change mitigation (Kavehei et al., 2018). Adopting tree species that excel in this regard can promote carbon neutrality at the city level (Rodriguez Mendez et al., 2024). While GI intervention is often used to address urban hazards, some areas do not suffer from significant urban hazards, providing potential spaces for maximizing the carbon sequestration capacity. Despite some disadvantages in other aspects, the fast growth rate of *Cedrus deodara* allows it to sequester more carbon, making it the most recommended species in Zone II and III where the urban problems are not prominent. Therefore, we propose the second GI intervention strategy: maximizing carbon sequestration potential in areas without pronounced urban hazards. The carbon sequestration of different tree species varies greatly. The proposed methodological framework can identify potential spaces and preferentially rank advantageous tree species in carbon sequestration. This approach supports the development of a rational GI planning strategy to maximize the contribution to carbon neutrality at the city level, extending the significance of GI planning beyond responding to urban hazards.

### 4.3. Limitations and future directions

In this study, as in numerous previous GI planning studies, the priority for GI intervention is simply determined by the spatial difference of urban hazards without considering policy and practical factors. These GI planning studies, however, only provide theoretically optimal scenarios without accounting for practical challenges, such as budget constraints, existing urban landscape characteristics and residents' willingness to pay (den Heijer and Coppens, 2023; Lu et al., 2022). Aligning practical implementation with the theoretically optimal schemes is a worthwhile direction that requires further exploration. Besides their ecological effectiveness, other characteristics of tree species, such as safety, aesthetics, and maintenance, should also be considered. We suggest fully accounting for these disadvantageous or restrictive factors of tree species by introducing penalty functions or constraints in future studies.

Furthermore, this study has limitations in quantifying local demands and effectiveness of tree species. For instance, although Landsat-derived LST is widely used and provides efficient coverage of large areas, it correlates poorly with ground-level heat exposure experienced by residents and is limited by fixed acquisition date (Yi et al., 2025). Follow-up studies could adopt more advanced demand indicators with a finer spatial and temporal resolution (e.g., Mean Radiant Temperature that better reflects actual pedestrian thermal experiences by incorporating fine-scale urban elements like building geometry, street trees, and ground surfaces that influence human comfort (Li et al., 2023). The i-Tree Eco model remains fundamentally empirical with inherent uncertainties; e.g., Lin et al. (2021) reported it generates approximately 11.1 % uncertainty when quantifying carbon sequestration. While the model has been adapted to support various regions globally, its foundation in North American tree growth equations and allometric data may produce additional uncertainty when applied to different geographic contexts. We recommend that upcoming studies employ more precise methodologies or validate the local accuracy of the i-Tree Eco model before implementation. In addition, GI planning strategies are determined by the conditions at a specific period. Nevertheless, the urban greening implementations are typically long-term projects, with planning periods for specific projects potentially extending over 5 years (Johnson and Handel, 2016; Liao et al., 2021). We propose that future exploration could continuously monitor and evaluate the planning outcomes to adapt strategies according to actual variations in ecological conditions.

## 5. Conclusions

In the context of climate change and urbanization, GI is an effective practice for enhancing cities' resilience and sustainability. Prior studies, while recognizing its multifunctionality, often focus primarily on determining prioritized locations. To address this limitation, we quantified the effectiveness of various tree species for GI intervention and developed an adaptive ranking approach to match their effectiveness with the locally-specific demands. A case study was conducted in the Chinese city of Zhengzhou, and the main conclusions are as follows:

(1) Locations in the urban core area, as well as the northwest, should be prioritized for GI intervention, with the southwest being given lower priority.
(2) Urban hazards exhibit significant spatial heterogeneity, and different tree species also have specific advantages, highlighting the importance of adaptive decision-making based on locally specific needs for GI intervention—essentially, planning the right GI in the right places.
(3) The study area is divided into three zones: the key GI intervention zone, the urban heat priority zone, and the air quality priority zone. *Acer truncatum*, *Magnolia grandiflora*, *Cedrus deodara* and *Fraxinus chinensis* are recommended for the three zones to respond to their specific urban hazards.

Based on the above findings, we propose two GI planning strategies: (1) targeting urban hazards with the most effective GI intervention and (2) maximizing carbon sequestration potential in areas without pronounced urban hazards. This framework offers a practical approach for the targeted placement of the right GI in the right locations, which could serve as guidance for decision-makers and urban planners in formulating effective urban greening programs.

## CRediT authorship contribution statement

**Dong Xinyu:** Writing – original draft, Visualization, Software, Methodology, Investigation, Formal analysis, Data curation, Conceptualization. **Ye Yanmei:** Writing – review & editing, Conceptualization. **Su Dan:** Software, Resources, Formal analysis, Data curation. **Yi Shengao:** Writing – review & editing, Visualization, Validation. **Yang Runjia:** Writing – review & editing, Formal analysis. **Haase Dagmar:** Writing – review & editing, Supervision. **Lausch Angela:** Writing – review & editing, Supervision.

## Declaration of Competing Interest

The authors declare that they have no known competing financial interests or personal relationships that could have appeared to influence the work reported in this paper.

## Acknowledgements

This research was financed by the National Social Science Foundation of China (19ZDA088) and the National Natural Science Foundation of China (72204101).

## Appendix A. Supporting information

Supplementary data associated with this article can be found in the online version at doi:10.1016/j.ufug.2025.128776.

## References

Alves, A., van Opstal, C., Keijzer, N., Sutton, N., Chen, W.-S., 2024. Planning the multifunctionality of nature-based solutions in urban spaces. Cities 146, 104751. https://doi.org/10.1016/j.cities.2023.104751.
Asaly, S., Gottlieb, L.-A., Yair, Y., Price, C., Reuveni, Y., 2023. Predicting Eastern Mediterranean Flash floods using support vector machines with precipitable water vapor, pressure, and lightning data. Remote Sens. 15. https://doi.org/10.3390/rs15112916.
Aydin, E.E., Ortner, F.P., Peng, S., Yenardi, A., Chen, Z., Tay, J.Z., 2024. Climate-responsive urban planning through generative models: sensitivity analysis of urban planning and design parameters for urban heat island in Singapore's residential settlements. Sustain. Cities Soc. 114, 105779. https://doi.org/10.1016/j.scs.2024.105779.
Bruner, S.G., Palmer, M.I., Griffin, K.L., Naeem, S., 2023. Planting design influences green infrastructure performance: plant species identity and complementarity in rain gardens. Ecol. Appl. 33, e2902. https://doi.org/10.1002/eap.2902.
Camacho-Caballero, D., Langemeyer, J., Segura-Barrero, R., Ventura, S., Beltran, A.M., Villalba, G., 2024. Assessing Nature-based solutions in the face of urban vulnerabilities: a multi-criteria decision approach. Sustain. Cities Soc. 103, 105257. https://doi.org/10.1016/j.scs.2024.105257.
Cao, F., Xu, X., Zhang, C., Kong, W., 2023. Evaluation of urban flood resilience and its space-time evolution: a case study of Zhejiang Province, China. Ecol. Indic. 154, 110643. https://doi.org/10.1016/j.ecolind.2023.110643.
Chang, H.-S., Lin, Z.-H., Hsu, Y.-Y., 2021. Planning for green infrastructure and mapping synergies and trade-offs: a case study in the Yanshuei River Basin, Taiwan. Urban For. Urban Green. 65, 127325. https://doi.org/10.1016/j.ufug.2021.127325.
Chen, H., Wang, N., Liu, Y., Zhang, Y., Lu, Y., Li, X., et al., 2022. A green infrastructure planning framework–guidance for priority, hubs and types. Urban For. Urban Green. 70, 127545. https://doi.org/10.1016/j.ufug.2022.127545.
Cook, A., Merwade, V., 2009. Effect of topographic data, geometric configuration and modeling approach on flood inundation mapping. J. Hydrol. 377, 131–142. https://doi.org/10.1016/j.jhydrol.2009.08.015.
Cook, L.M., Good, K.D., Moretti, M., Kremer, P., Wadzuk, B., Traver, R., et al., 2024. Towards the intentional multifunctionality of urban green infrastructure: a paradox of choice? npj Urban Sustain. 4, 12. https://doi.org/10.1038/s42949-024-00145-0.
Corgo, J., Cruz, S.S., Conceição, P., 2024. Nature-based solutions in spatial planning and policies for climate change adaptation: a literature review. Ambio. https://doi.org/10.1007/s13280-024-02052-1.
den Heijer, C., Coppens, T., 2023. Paying for green: a scoping review of alternative financing models for nature-based solutions. J. Environ. Manag. 337, 117754. https://doi.org/10.1016/j.jenvman.2023.117754.
Dong, X., Yang, R., Ye, Y., Cui, L., 2023a. Trade-off efficiency: linking urban socioecological quality with land use efficiency from return on investment perspective. Sustain. Cities Soc. 99, 104968. https://doi.org/10.1016/j.scs.2023.104968.
Dong, X., Ye, Y., Yang, R., Li, X., 2023b. Planning for green infrastructure based on integration of multi-driving factors: A case study in pilot site of sponge city. Sustain. Cities Soc. 93, 104549. https://doi.org/10.1016/j.scs.2023.104549.
Dong, X., Yi, W., Yuan, P., Song, Y., 2023c. Optimization and trade-off framework for coupled green-grey infrastructure considering environmental performance. J. Environ. Manag. 329, 117041. https://doi.org/10.1016/j.jenvman.2022.117041.
Getirana, A., Mandarino, F., Ney de Montezuma, P., Kirschbaum, D., 2023. An urban drainage scheme for large-scale flood models. J. Hydrol. 627, 130410. https://doi.org/10.1016/j.jhydrol.2023.130410.
Goodspeed, R., Liu, R., Gounaridis, D., Lizundia, C., Newell, J., 2021. A regional spatial planning model for multifunctional green infrastructure. Environ. Plan. B: Urban Anal. City Sci. 49, 815–833. https://doi.org/10.1177/23998083211033610.
Guo, X., Cheng, J., Yin, C., Li, Q., Chen, R., Fang, J., 2023. The extraordinary Zhengzhou flood of 7/20, 2021: how extreme weather and human response compounding to the disaster. Cities 134, 104168. https://doi.org/10.1016/j.cities.2022.104168.
i-Tree. i-Tree ECO User's Manual. Available online: https://www.itreetools.org (accessed on October 2024).
Jia, H., Liu, Z., Xu, C., Chen, Z., Zhang, X., Xia, J., et al., 2022. Adaptive pressure-driven multi-criteria spatial decision-making for a targeted placement of green and grey runoff control infrastructures. Water Res. 212, 118126. https://doi.org/10.1016/j.watres.2022.118126.
Johnson, L.R., Handel, S.N., 2016. Restoration treatments in urban park forests drive long-term changes in vegetation trajectories. Ecol. Appl. 26, 940–956. https://doi.org/10.1890/14-2063.
Kavehei, E., Jenkins, G.A., Adame, M.F., Lemckert, C., 2018. Carbon sequestration potential for mitigating the carbon footprint of green stormwater infrastructure. Renew. Sustain. Energy Rev. 94, 1179–1191. https://doi.org/10.1016/j.rser.2018.07.002.
Korkou, M., Tarigan, A.K.M., Hanslin, H.M., 2023. The multifunctionality concept in urban green infrastructure planning: A systematic literature review. Urban For. Urban Green. 85, 127975. https://doi.org/10.1016/j.ufug.2023.127975.
Leng, L., Jia, H., Xu, C., 2024. Incorporating spatial heterogeneity information into multi-objective optimization methodology of green infrastructure. J. Clean. Prod. 468, 143060. https://doi.org/10.1016/j.jclepro.2024.143060.
Lin, J., Kroll, C.N., Nowak, D.J., 2021. An uncertainty framework for i-Tree eco: a comparative study of 15 cities across the United States. Urban For. Urban Green. 60, 127062. https://doi.org/10.1016/j.ufug.2021.127062.
Li, H., Jombach, S., Tian, G., Li, Y., Meng, H., 2022. Characterizing temporal dynamics of urban heat island in a rapidly expanding city: a 39 years study in Zhengzhou, China. Land 11. https://doi.org/10.3390/land11101838.
Li, S., Zhao, Y., Xiao, W., Yue, W., Wu, T., 2021. Optimizing ecological security pattern in the coal resource-based city: a case study in Shuozhou City, China. Ecol. Indic. 130, 108026. https://doi.org/10.1016/j.ecolind.2021.108026.
Li, X., Chakraborty, T.C., Wang, G., 2023. Comparing land surface temperature and mean radiant temperature for urban heat mapping in Philadelphia. Urban Clim. 51, 101615. https://doi.org/10.1016/j.uclim.2023.101615.
Li, Y., Zhang, X., Xia, C., 2023. Towards a greening city: how does regional cooperation promote urban green space in the Guangdong-Hong Kong-Macau Greater Bay Area? Urban For. Urban Green. 86, 128033. https://doi.org/10.1016/j.ufug.2023.128033.
Liao, L., Zhao, C., Li, X., Qin, J., 2021. Towards low carbon development: the role of forest city constructions in China. Ecol. Indic. 131, 108199. https://doi.org/10.1016/j.ecolind.2021.108199.
Liu, F., Zhang, Z., Shi, L., Zhao, X., Xu, J., Yi, L., et al., 2016. Urban expansion in China and its spatial-temporal differences over the past four decades. J. Geogr. Sci. 26, 1477–1496. https://doi.org/10.1007/s11442-016-1339-3.
Lombardía, A., Gómez-Villarino, M.T., 2023. Green infrastructure in cities for the achievement of the un sustainable development goals: a systematic review. Urban Ecosyst. 26, 1693–1707. https://doi.org/10.1007/s11252-023-01401-4.

Lu, Y., Rigolon, A., Carver, S., Wu, J., 2024. Data augmented planning: a data-driven approach to measuring-understanding-optimizing green justice across 263 Chinese cities. Sustain. Cities Soc. 117, 105981. https://doi.org/10.1016/j.scs.2024.105981.

Lu, Y., Xu, S., Liu, S., Wu, J., 2022. An approach to urban landscape character assessment: linking urban big data and machine learning. Sustain. Cities Soc. 83, 103983. https://doi.org/10.1016/j.scs.2022.103983.

Maji, K.J., Namdeo, A., Bramwell, L., 2023. Driving factors behind the continuous increase of long-term PM2.5-attributable health burden in India using the high-resolution global datasets from 2001 to 2020. Sci. Total Environ. 866, 161435. https://doi.org/10.1016/j.scitotenv.2023.161435.

Manzini, J., Hoshika, Y., Carrari, E., Sicard, P., Watanabe, M., Tanaka, R., et al., 2023. FlorTree: a unifying modelling framework for estimating the species-specific pollution removal by individual trees and shrubs. Urban For. Urban Green. 85, 127967. https://doi.org/10.1016/j.ufug.2023.127967.

Martilli, A., Krayenhoff, E.S., Nazarian, N., 2020. Is the urban heat island intensity relevant for heat mitigation studies? Urban Clim. 31, 100541. https://doi.org/10.1016/j.uclim.2019.100541.

Meerow, S., 2019. A green infrastructure spatial planning model for evaluating ecosystem service tradeoffs and synergies across three coastal megacities. Environ. Res. Lett. 14, 125011. https://doi.org/10.1088/1748-9326/ab502c.

Meerow, S., 2020. The politics of multifunctional green infrastructure planning in New York City. Cities 100, 102621. https://doi.org/10.1016/j.cities.2020.102621.

Meerow, S., Newell, J.P., 2017. Spatial planning for multifunctional green infrastructure: growing resilience in Detroit. Landsc. Urban Plan. 159, 62–75. https://doi.org/10.1016/j.landurbplan.2016.10.005.

MOHURD, 2023. Ministry of Housing and Urban-Rural Development abbreviation: Announcement on the publication of the industry standard 'Urban Road Greening Design Standards' Available online: https://www.gov.cn/zhengce/zhengceku/202311/content_6916049.htm (accessed on July 2024).

Morakinyo, T.E., Lau, K.K.-L., Ren, C., Ng, E., 2018. Performance of Hong Kong's common trees species for outdoor temperature regulation, thermal comfort and energy saving. Build. Environ. 137, 157–170. https://doi.org/10.1016/j.buildenv.2018.04.012.

Nyelele, C., Kroll, C.N., Nowak, D.J., 2022. A comparison of tree planting prioritization frameworks: i-tree landscape versus spatial decision support tool. Urban For. Urban Green. 75, 127703. https://doi.org/10.1016/j.ufug.2022.127703.

Ortega, U., Ametzaga-Arregi, I., Sertutxa, U., Peña, L., 2023. Identifying a green infrastructure to prioritise areas for restoration to enhance the landscape connectivity and the provision of ecosystem services. Landsc. Ecol. 38, 3751–3765. https://doi.org/10.1007/s10980-023-01789-6.

Oshio, H., Kiyono, T., Asawa, T., 2021. Numerical simulation of the nocturnal cooling effect of urban trees considering the leaf area density distribution. Urban For. Urban Green. 66, 127391. https://doi.org/10.1016/j.ufug.2021.127391.

Pugliese Viloria, A.D., Folini, A., Carrion, D., Brovelli, M.A., 2024. Hazard susceptibility mapping with machine and deep learning: a literature review. Remote Sens. 16. https://doi.org/10.3390/rs16183374.

Rainey, W., McHale, M., Arabi, M., 2022. Characterization of co-benefits of green stormwater infrastructure across ecohydrologic regions in the United States. Urban For. Urban Green. 70, 127514. https://doi.org/10.1016/j.ufug.2022.127514.

Riondato, E., Pilla, F., Sarkar Basu, A., Basu, B., 2020. Investigating the effect of trees on urban quality in Dublin by combining air monitoring with i-tree eco model. Sustain. Cities Soc. 61, 102356. https://doi.org/10.1016/j.scs.2020.102356.

Ristorini, M., Guidolotti, G., Sgrigna, G., Jafari, M., Knappe, D., Garfì, V., et al., 2023. Nature-based solutions in post-industrial sites: Integrated evaluation of atmospheric pollution abatement and carbon uptake in a German city. Urban Clim. 50, 101579. https://doi.org/10.1016/j.uclim.2023.101579.

Rodriguez Mendez, Q., Fuss, S., Lück, S., Creutzig, F., 2024. Assessing global urban CO2 removal. Nat. Cities 1, 413–423. https://doi.org/10.1038/s44284-024-00069-x.

Salmond, J.A., Tadaki, M., Vardoulakis, S., Arbuthnott, K., Coutts, A., Demuzere, M., et al., 2016. Health and climate related ecosystem services provided by street trees in the urban environment. Environ. Health 15, S36. https://doi.org/10.1186/s12940-016-0103-6.

Sarabi, S., Han, Q., de Vries, B., Romme, A.G.L., 2022. The nature-based solutions planning support system: a playground for site and solution prioritization. Sustain. Cities Soc. 78, 103608. https://doi.org/10.1016/j.scs.2021.103608.

Schneider, A., Mertes, C.M., 2014. Expansion and growth in Chinese cities, 1978–2010. Environ. Res. Lett. 9, 024008. https://doi.org/10.1088/1748-9326/9/2/024008.

Sekertekin, A., Bonafoni, S., 2020. Land surface temperature retrieval from landsat 5, 7, and 8 over rural areas: assessment of different retrieval algorithms and emissivity models and toolbox implementation. Remote Sens. 12. https://doi.org/10.3390/rs12020294.

Shen, S., Li, C., van Donkelaar, A., Jacobs, N., Wang, C., Martin, R.V., 2024. Enhancing global estimation of fine particulate matter concentrations by including geophysical a priori information in deep learning. ACS EST Air 1, 332–345. https://doi.org/10.1021/acsestair.3c00054.

Tran, T.J., Helmus, M.R., Behm, J.E., 2020. Green infrastructure space and traits (GIST) model: integrating green infrastructure spatial placement and plant traits to maximize multifunctionality. Urban For. Urban Green. 49, 126635. https://doi.org/10.1016/j.ufug.2020.126635.

USGS, 2024. Landsat Collection 2 Level-2 Science Products. Available online: https://www.usgs.gov/landsat-missions/landsat-collection-2-level-2-science-products (accessed on October 2024).

Van Oijstaeijen, W., Van Passel, S., Cools, J., 2020. Urban green infrastructure: a review on valuation toolkits from an urban planning perspective. J. Environ. Manag. 267, 110603. https://doi.org/10.1016/j.jenvman.2020.110603.

Wang, S., Yin, S., Zhang, R., Yang, L., Zhao, Q., Zhang, L., et al., 2019. Insight into the formation of secondary inorganic aerosol based on high-time-resolution data during haze episodes and snowfall periods in Zhengzhou, China. Sci. Total Environ. 660, 47–56. https://doi.org/10.1016/j.scitotenv.2018.12.465.

Wang, Y., Chang, Q., Fan, P., 2021. A framework to integrate multifunctionality analyses into green infrastructure planning. Landsc. Ecol. 36, 1951–1969. https://doi.org/10.1007/s10980-020-01058-w.

Xu, C., Huang, Q., Haase, D., Dong, Q., Teng, Y., Su, M., et al., 2024. Cooling effect of green spaces on urban heat island in a chinese megacity: increasing coverage versus optimizing spatial distribution. Environ. Sci. Technol. 58, 5811–5820. https://doi.org/10.1021/acs.est.3c11048.

Yang, H., Wu, Z., Dawson, R.J., Barr, S., Ford, A., Li, Y., 2024. Quantifying surface urban heat island variations and patterns: Comparison of two cities in three-stage dynamic rural–urban transition. Sustain. Cities Soc. 109, 105538. https://doi.org/10.1016/j.scs.2024.105538.

Yang, Q., Huang, X., Tang, Q., 2019. The footprint of urban heat island effect in 302 Chinese cities: temporal trends and associated factors. Sci. Total Environ. 655, 652–662. https://doi.org/10.1016/j.scitotenv.2018.11.171.

Yang, Q., Yuan, Q., Li, T., Yue, L., 2020. Mapping PM2.5 concentration at high resolution using a cascade random forest based downscaling model: evaluation and application. J. Clean. Prod. 277, 123887. https://doi.org/10.1016/j.jclepro.2020.123887.

Yao, Y., Wang, Y., Ni, Z., Chen, S., Xia, B., 2022. Improving air quality in Guangzhou with urban green infrastructure planning: an i-TRee Eco Model Study. J. Clean. Prod. 369, 133372. https://doi.org/10.1016/j.jclepro.2022.133372.

Yi, S., Li, X., Ma, C., Wang, R., Zhou, Y., Xu, Q., et al., 2025. Assessing the differential impact of vegetated and built-up areas on heat exposure environment: a case study of Los Angeles. Build. Environ. 271, 112538. https://doi.org/10.1016/j.buildenv.2025.112538.

Yin, D., Chen, Y., Jia, H., Wang, Q., Chen, Z., Xu, C., et al., 2021. Sponge city practice in China: a review of construction, assessment, operational and maintenance. J. Clean. Prod. 280, 124963. https://doi.org/10.1016/j.jclepro.2020.124963.

Zhang, Z., Zhao, W., Liu, Y., Pereira, P., 2023. Impacts of urbanisation on vegetation dynamics in Chinese cities. Environ. Impact Assess. Rev. 103, 107227. https://doi.org/10.1016/j.eiar.2023.107227.

Zhao, H., Zhao, D., Jiang, X., Zhang, S., Lin, Z., 2023a. Assessment of Urban Forest Ecological Benefit Based on the i-Tree Eco Model—A Case Study of Changchun Central City. Forests 14. https://doi.org/10.3390/f14071304.

Zhao, W., Zhou, A., Yin, C., 2023b. Unraveling the research trend of ecological civilization and sustainable development: a bibliometric analysis. Ambio 52, 1928–1938. https://doi.org/10.1007/s13280-023-01947-9.

Zhou, Q., Konijnendijk van den Bosch, C.C., Chen, Z., Wang, X., Zhu, L., Chen, J., et al., 2021. China's Green space system planning: development, experiences, and characteristics. Urban For. Urban Green. 60, 127017. https://doi.org/10.1016/j.ufug.2021.127017.

Zhu, X., Guo, H., Huang, J.J., 2024. Urban flood susceptibility mapping using remote sensing, social sensing and an ensemble machine learning model. Sustain. Cities Soc. 108, 105508. https://doi.org/10.1016/j.scs.2024.105508.